Effects of A desorption on the first-order transition in the A-B_2 reaction model

Benjamin J. Brosilow and Robert M. Ziff
Department of Chemical Engineering, The University of Michigan, Ann Arbor, Michigan 48109-2136
(Received 14 January 1992)

The A-B_2 surface-reaction model [R. M. Ziff, E. Gulari, and Y. Barshad, Phys. Rev. Lett. **56**, 2553 (1986)] is studied including spontaneous desorption of CO from the catalyst surface. It is found that when the spontaneous desorption probability P is above a critical value $P_c > 0.039$, the system no longer exhibits a first-order kinetic phase transition. The interface between coexisting phases is found to be nonfractal for P below P_c, but it becomes fractal with dimension $D = 1.46 \pm 0.05$ when $P = P_c$. The critical behavior of the model is qualitatively described by Dickman's one-site mean-field approximation.

PACS number(s): 05.70.Ln, 82.20.Mj, 05.70.Jk, 82.65.Jv

I. INTRODUCTION

It is known that nonequilibrium systems can exhibit behavior similar to phase transitions seen in equilibrium systems [1,2]. Recently, Ziff, Gulari, and Barshad (ZGB) introduced a nonequilibrium model of surface reaction which shows such kinetic phase transitions [3]. This model describes the heterogeneous catalytic reaction of carbon monoxide and oxygen over a platinum crystal, and has become known as the ZGB or A-B_2 model (A denoting CO and B_2 denoting oxygen). In this paper we investigate an extension of this model previously considered by Ehsasi *et al.* [4] and Kaukonen and Nieminen [5], in which an A-desorption step is incorporated. In particular, we investigate the effects of this desorption on the behavior of the first-order kinetic phase transition.

II. MODEL

A detailed description of the ZGB model can be found in Ref. [3], so we present only a brief description here. In the model's simplest form, surface diffusion, spontaneous desorption, and thermal effects are ignored. The catalyst surface is modeled by a two-dimensional square lattice, onto which molecules attempt to adsorb one at a time with random position. A molecules require one vacant site to adsorb, while B_2 molecules require two adjacent vacant sites. The temperature and pressure of the system are assumed to be such that the kinetics are adsorption limited, so that nearest-neighbor pairs of A and B react and desorb immediately upon formation. The only parameter in the model is y, defined as the probability that a molecule making an adsorption attempt is an A.

Two different algorithms have been used to simulate the ZGB model, the constant-y (C-y) algorithm and the constant-coverage (C-Θ) algorithm. In the C-y algorithm [3], a fixed value is chosen for y prior to beginning the simulation. At each time step, an A adsorption is attempted with probability y, or otherwise a B_2 adsorption is attempted. If an A adsorption is attempted, then a random lattice site is chosen, and if the site is unoccupied, an A molecule is placed at the site. If the site is occupied, then no change in the state of the lattice occurs at this time step. In the case of B_2 adsorption, a random nearest-neighbor pair of lattice sites is chosen, and if both sites are vacant, then a B atom is placed on each site. If either or both of the sites are occupied, then no change in the state of the lattice occurs at this time step. After each adsorption of an A or B_2 molecule, the neighboring lattice sites are checked in a random order for the existence of A-B nearest neighbors. If such a pair is found, then the A and B molecules desorb from the surface (as AB), leaving behind two vacant lattice sites. One Monte Carlo step (MCS) is said to have elapsed after the number of time steps equals the number of sites on the lattice.

In the C-Θ algorithm, which was recently proposed by the authors [6], a fixed value Θ_A is chosen as the set point for the coverage of species A before the simulation is run. The choice of which species will attempt an adsorption at a particular time step is made according to the following deterministic rule: When the instantaneous coverage of species A (denoted Θ') is greater than the set-point value Θ_A, then only B_2 adsorptions are attempted. When $\Theta' \leq \Theta_A$ then only A adsorptions are attempted. The rest of the procedure—picking one or two sites, checking that they are vacant, and checking neighbors for reactions—remains the same as in the C-y algorithm. The total number of A and B adsorption attempts are counted, and y is defined as the fraction of the attempts where the adsorbing particle is an A.

Simulations of the ZGB model using the C-y algorithm [3–5,7–17] show that after many Monte Carlo steps, the system reaches a steady state where the average fractional coverage of A and B (denoted Θ_A and Θ_B, respectively) remain roughly constant. For $y < y_1 \approx 0.3907$ [17] the surface achieves a B-saturated steady state in which every site is occupied by B, and no reaction can occur. For $y_1 < y < y_2 \approx 0.525\,60$ [6] the system achieves a steady state in which the surface is occupied by both A and B, separated by vacant sites. Steady-state reaction occurs only in this region. For $y > y_2$, the surface achieves an A-saturated steady state where every lattice site is occupied A, and again, no reaction occurs at steady state in this region. The transition to the A-saturated state at y_2 is first order, in that Θ_A and Θ_B change discontinuously with a change in y. The transition from the B-saturated state at y_1 is second order, since the derivative of the change in surface coverage is discontinuous with a change in y.

Simulations of the ZGB model using the C-Θ algorithm produce the same relationship between y, Θ_A, and Θ_B seen in the C-y algorithm, except that the first-order transition at y_2 is replaced by a metastability loop. The states represented by this metastability loop have been shown to be metastable and unstable steady states of the C-y algorithm [6].

The relationship between the two algorithms can be seen as follows: In the C-Θ algorithm there is a correlation between the type of species attempting an adsorption at one time step and the type of species attempting an adsorption at the next time step, while no such correlation exists in the C-y algorithm. The correlation is present in the C-Θ algorithm because when $\Theta' > \Theta_A$, there will likely be many B_2 adsorption attempts before a B_2 molecule successfully adsorbs and reacts, and similarly for A adsorption attempts when $\Theta' \leq \Theta_A$. Note, however, that if one considers only a very small region on the lattice in a C-Θ algorithm, then on this region there will be no temporal correlation between the types of particles attempting to adsorb, since it is unlikely that successive adsorption attempts will fall in the same small region of the lattice. Thus, if one considers the simulation from the perspective of a sufficiently small region of the catalyst surface, the two algorithms are indistinguishable. Hence each small region of the lattice must behave in a way that is consistent with both algorithms operating at the average or constant value of y.

III. DESORPTION OF SPECIES A

Initial investigations into the effects of A-desorption in the ZGB model were independent studies by Ehsasi *et al.* [4] and Kaukonen and Nieminen [5]. The two groups incorporated A desorption into the model in slightly different but equivalent ways, and we have adopted the method of Ehsasi *et al.* In this method the C-y algorithm is run as usual, but after each adsorption attempt, a site is chosen at random, and if occupied by A, the site is made vacant with probability P. This results in a rate of desorption $r_{\text{des}} = P\Theta_A$ molecules per MCS per lattice site.

For low values of P, both studies found that the transition value y_2 increases with increasing P. Also, the surface remains reactive for $y > y_2$, since A desorption creates vacant sites where reaction can occur. Thus the first-order transition at y_2 is now between a low-Θ_A state and a high-Θ_A state, both of which are reactive (as opposed to the case with no desorption, where the transition is between a reactive, low-Θ_A state and an adsorbing state where every site is occupied by A).

Kaukonen and Nieminen noted in their work that as the value of P is increased beyond some critical value P_c, the first-order transition at y_2 seems to disappear. From their published results it is difficult to estimate the value of P_c. However, from the results of Ehsasi *et al.* (Fig. 11 in Ref. [4]), which also imply the existence of such a critical value, one can estimate $0.03 < P_c < 0.25$.

We ran simulations of the model with A desorption, making use of the C-Θ algorithm. Because the C-Θ algorithm has no instability at the first-order transition, we were able to collect more data near the transition than was possible in either of the previous studies. Our results are consistent with those of Ehsasi *et al.* and Kaukonen and Nieminen, but are of higher precision. These results are shown in Fig. 1. For $P \leq 0.03$, a metastability loop was found, implying the existence of a phase transition. (The loop is, however, too small to be seen in the figure.) For $P \geq 0.05$, no metastability loop was found, and thus we conclude that $0.03 < P_c < 0.05$. It is interesting to note that P affects the curves of Fig. 1 in a way that is similar to the effect of temperature on the curves of a PVT diagram for a fluid near its critical point.

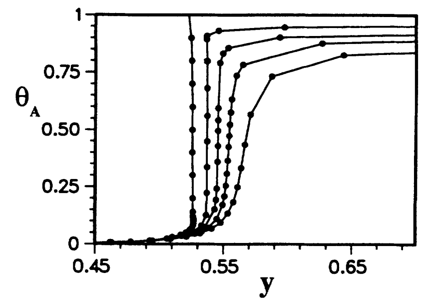

FIG. 1. The phase diagram for the ZGB model with desorption probability P. The curves correspond, from left to right, to $P = 0$, 0.03, 0.05, 0.07, and 0.10. Each dot represents the results of a separate simulation using the C-Θ algorithm.

IV. FRACTAL SCALING OF THE INTERFACE BETWEEN PHASES IN EQUILIBRIUM

The next series of simulations that we ran were directed at characterizing the fractal properties of the interface between the two phases present at the first-order transition. These simulations involved running the C-Θ algorithm on a lattice of $L \times W$ sites with periodic boundary conditions. The initial state of the lattice was an $L/2 \times W$ rectangle of adsorbed A, with the other sites initially vacant. The simulations were run with $\Theta_A = 0.5$. Figure 2(a) shows a snapshot of a lattice with $L = W = 1024$ sites after the simulation was run for 236 000 MCS at $P = 0$. A clear separation exists between the high-Θ_A and low-Θ_A phases. Figures 2(b)–2(e) show that as P is increased, the phases seem to mix, until there is no longer any sign of phase separation by $P \approx 0.05$. This phenomenon is reminiscent of the disappearance of surface tension as a fluid passes through its critical point.

To determine the fractal properties of the phase boundary, we carried out the following procedure: An interface between phases was defined as a path of A-occupied sites that wrapped around the periodic boundary in the vertical direction (as oriented in Fig. 2), and along which one could walk, always keeping vacant sites to the left (as shown in Fig. 3). Each $L \times W$ system was initialized for a period during which the phase interface was checked every 3000 MCS. If an interface was found, then its length (defined as the length of the walk along the boundary) and width (defined as the standard deviation of the

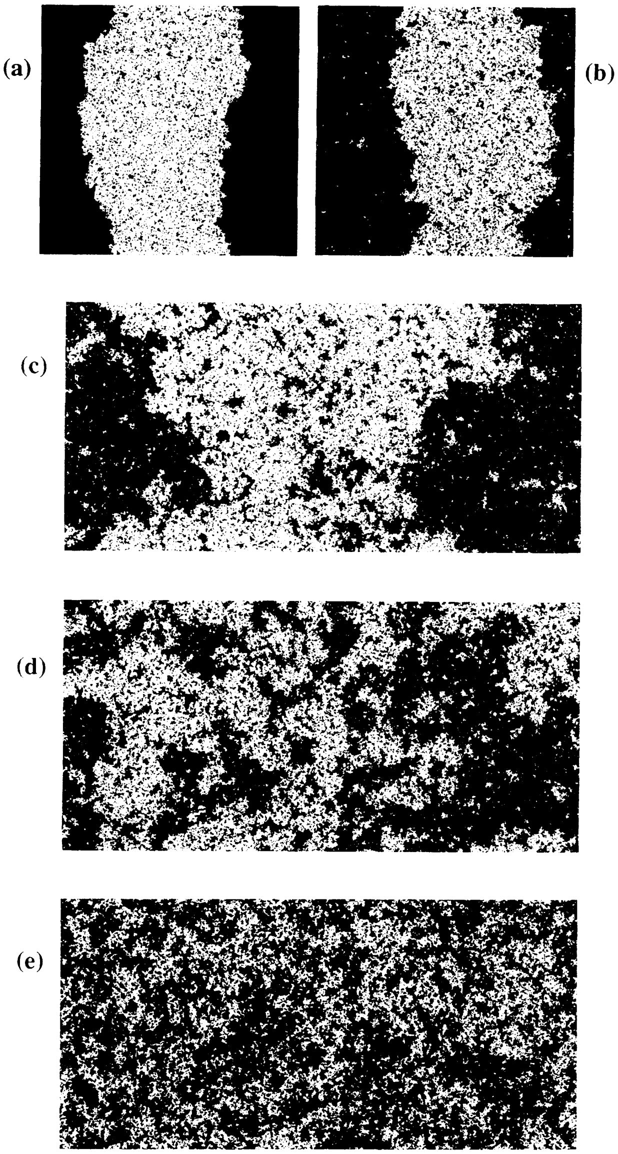

FIG. 2. Snapshots of typical configurations of the catalyst surface for runs of the C-Θ algorithm as described in the text. Black dots represent adsorbed A. Adsorbed B and vacant sites are not shown. (a) 1024×1024 lattice with $P=0$. (b) 1024×1024 lattice with $P=0.030$. (c) 2048×1024 lattice with $P=0.039$. (d) 2048×1024 lattice with $P=0.041$. (e) 2048×1024 lattice with $P=0.050$. The lattices are longer for P near the critical point in order to accommodate larger fluctuations in the phase interface.

horizontal coordinates of the sites on the interface) were measured. When these two parameters stopped increasing consistently and began fluctuating randomly (which typically took from 50 000 to 150 000 MCS to occur), we began taking measurements of the fractal dimension, repeating at 500 MCS intervals. Each measurement was made by choosing a lattice point on the interface to be at the center of a coordinate system, and then finding the length of the interface that fell within a circular region of radius R about this central point, for values of R from 1 to $W/2$ sites. This calculation was then repeated with a

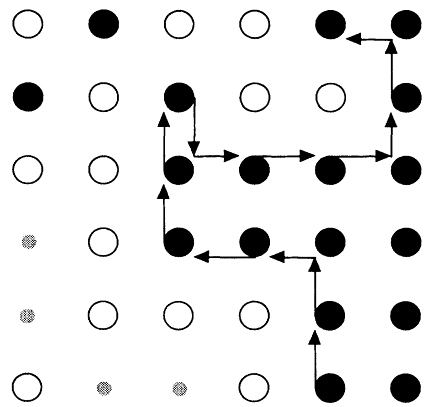

FIG. 3. The arrows show a walk that defines a small section of a sample phase interface, as described in the text. Black dots are adsorbed A, open circles are vacant sites, and small grey dots are adsorbed B. For a walker moving in the direction of the arrows, vacant sites are always to the left, and adsorbed A is always to the right.

new point on the interface serving as the central point, until each point on the interface had served as a center. These results are plotted in Fig. 4. To reduce the systematic scatter due to the use of circular shells on a discrete square lattice, these data were plotted as a function of $R_{\text{eff}}\equiv\sqrt{N/\pi}$, where N is the total number of lattice sites inside a circle of radius R. The use of R_{eff} results in much smoother curves for small R.

Of course, not all values of P produced systems where a phase interface could be found every time a search was made, so the data of Fig. 4 is an average over only those states where an interface could be found. For $P\leq0.039$, it was always possible to find the interface between the two phases, but for $P=0.040$ the interface was well defined only about 95% of the time. For $P=0.045$ the

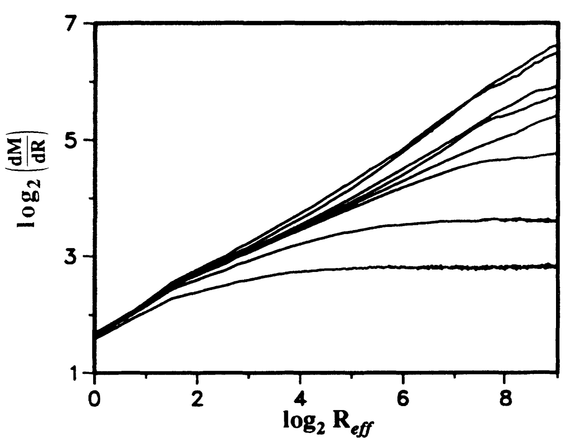

FIG. 4. A base-2 log-log plot of dM/dR vs R_{eff}, where M is the length of the phase interface inside a circle of radius R, and R_{eff} is the effective radius defined in the text. The curves correspond, from bottom to top, to $P=0$, 0.030, 0.039, 0.040, 0.041, 0.042, 0.045, and 0.050. The fractal dimension D of the interface for each P is given by $D=m+1$, where m is the slope of the curve in this plot.

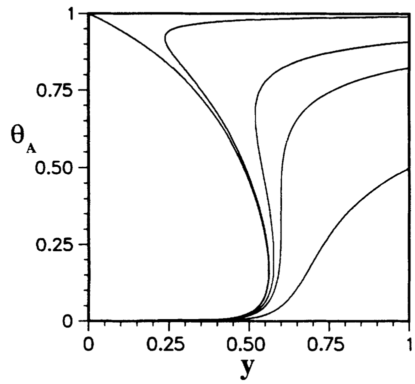

FIG. 5. The solution of the modified one-site approximation, Eqs. (1) and (2) in the text. The curves correspond, from left to right, to $P=0, 0.01, 0.1, 0.214$, and 1.0.

interface was defined a little less than half the time. Note that the snapshot shown in Fig. 2(e) does in fact have a continuous interface, even though there is no clear phase separation.

The slope m of the curves in Fig. 4 is related to the fractal dimension of the interface by $D=m+1$. From the figure one can see that for $P\leq 0.039$ the interface is nonfractal ($D=1$) for sufficiently large R, while for $P\geq 0.040$ the interface remains fractal ($D>1$) for R as large as the width of the system. This behavior is reminiscent of the behavior of an equilibrium fluid, where the correlation length diverges as the system approaches its critical point. By extension from equilibrium systems, we assume that the interface between the two phases in our system becomes fractal on all length scales at the critical point, and conclude that $P_c>0.039$. From the slope of the curves of Fig. 4, we find that for $P=0.040$ the interface has dimension $D=1.41$, for $P=0.041$ the interface has dimension $D=1.44$, and for $P=0.042$ the interface has dimension $D=1.51$. Averaging these results, we find that the fractal dimension of the interface at the critical point is $D=1.46\pm 0.05$.

Simultaneous to our work, Tomé and Dickman [18] also performed an investigation on this system to find the value of P_c. They made use of the C-y algorithm exclusively, and report a value $P_c\approx 0.04$, consistent with our results.

As mentioned previously, all the simulations described in this section were run with $\Theta_A=0.5$. This value of Θ_A was chosen as a rough approximation to $\Theta_{A,c}$, the coverage of species A at the critical point. We arrived at this approximation for $\Theta_{A,c}$ as follows: In Fig. 1, the curve for $P=0.03$ has a metastability loop with negative slope in the region $0.08\lesssim\Theta_A\lesssim 0.89$, while the curve for $P=0.05$ shows no metastability loop (i.e., the slope is positive everywhere). Since the presence of a metastability loop along a line of constant P indicates a phase separation, the two-phase envelope for this system must intersect the curve for $P=0.03$ at $\Theta_A\approx 0.08$ and 0.89, without intersecting the curve for $P=0.05$. Therefore the two-phase envelope must have extremely steep slope and low curvature for $0.08\lesssim\Theta_A\lesssim 0.89$, and $\Theta_{A,c}$ must fall within this range of Θ_A, i.e., $0.08\lesssim\Theta_{A,c}\lesssim 0.89$. We take the midpoint of this range, $\Theta_A\approx 0.5$, as our approximation to $\Theta_{A,c}$ for these simulations. We expect that this approximate value will be sufficient to produce critical behavior in our system since the low curvature of the two-phase envelope near the critical point should cause the system to show critical behavior for all Θ_A within a large neighborhood about $\Theta_{A,c}$. As demonstrated in Figs. 2(a)–2(e) and 4, this approximation is indeed sufficient, since in Fig. 2 we see that the two phases mix as P is increased (rather than one phase taking over the system as would be the case away from the critical point), and in Fig. 4 we find the fractal behavior expected near a critical point.

V. MEAN-FIELD APPROXIMATION

Dickman's one-site mean-field approximation to the ZGB model [19] can be modified to account for the desorption of species A. The resulting equations are

$$\frac{d\Theta_B}{dt}=2(1-y)\Theta_v^2(1-\Theta_A)^3-y\Theta_v[1-(1-\Theta_B)^4]\ , \qquad (1)$$

$$\frac{d\Theta_A}{dt}=-2(1-y)\Theta_v^2[1-(1-\Theta_A)^3] +y\Theta_v(1-\Theta_B)^4-P\Theta_A\ , \qquad (2)$$

with $\Theta_v=1-\Theta_A-\Theta_B$. We numerically solved these equations at steady state for Θ_A and Θ_B as a function of y, and found that $P_c\approx 0.214$ is the lowest value of P which does not produce a metastability loop (Fig. 5). Thus the one-site mean-field approximation predicts critical behavior for this system, although at a somewhat high desorption probability. An in-depth study of the effects of incorporating spontaneous desorption in the one-site mean-field approximation has been performed by Fischer and Titulaer [20].

VI. CONCLUSIONS

The addition of a probability P for the spontaneous desorption of species A adds richness to the first-order transition in the ZGB model. The effect on the model of varying P is similar to the effect of varying temperature in equilibrium systems with first-order phase transitions. The model exhibits critical-like behavior at $P=P_c>0.039$. The interface between the high- and low-Θ_A phases is fractal only at the critical desorption probability, with dimension $D=1.46\pm 0.05$.

ACKNOWLEDGMENTS

The authors thank R. Dickman and T. Tomé for making their results available to us prior to publication, and acknowledge support from the U.S. National Science Foundation, Grant No. DMR 8619731.

[1] See, for example, F. Schlögl, Z. Phys. **253**, 147 (1972); Phys. Rep. **62**, 267 (1980).
[2] H. Haken, *Synergetics* (Springer, Berlin, 1983).
[3] R. M. Ziff, E. Gulari, and Y. Barshad, Phys. Rev. Lett. **56**, 2553 (1986).
[4] M. Ehsasi, M. Matloch, O. Frank, J. H. Block, K. Christmann, F. S. Rys, and W. Hirschwald, J. Chem. Phys. **91**, 4949 (1989).
[5] H. P. Kaukonen and R. M. Nieminen, J. Chem. Phys. **91**, 4380 (1989).
[6] R. M. Ziff and B. J. Brosilow, Phys. Rev. A **46**, 4630 (1992).
[7] E. V. Albano, J. Chem. Phys. **94**, 1499 (1991).
[8] J. W. Evans and M. S. Miesch, Phys. Rev. Lett. **66**, 833 (1991).
[9] B. Yu, D. A. Browne, and P. Kleban, Phys. Rev. A **43**, 1770 (1991).
[10] R. Imbihl, A. E. Reynolds, and D. Kaletta, Phys. Rev. Lett. **67**, 275 (1991).
[11] P. Araya, W. Porod, and E. E. Wolf, Surf. Sci. **230**, 245 (1990).
[12] P. Meakin, J. Chem. Phys. **93**, 2903 (1990).
[13] M. Kolb and Y. Boudeville, J. Chem. Phys. **92**, 3935 (1990).
[14] G. Grinstein, Z. W. Lai, and D. A. Browne, Phys. Rev. A **40**, 4820 (1989).
[15] J. Mai, W. von Niessen, and A. Blumen, J. Chem. Phys. **93**, 3685 (1990).
[16] A. Sadiq, Z. Phys. B **67**, 221 (1987).
[17] I. Jensen, H. C. Fogedby, R. Dickman, Phys. Rev. A **41**, 3411 (1990).
[18] T. Tomé and R. Dickman (unpublished).
[19] R. Dickman, Phys. Rev. A **34**, 4246 (1986).
[20] P. Fischer and U. M. Titulaer, Surf. Sci. **221**, 409 (1989).

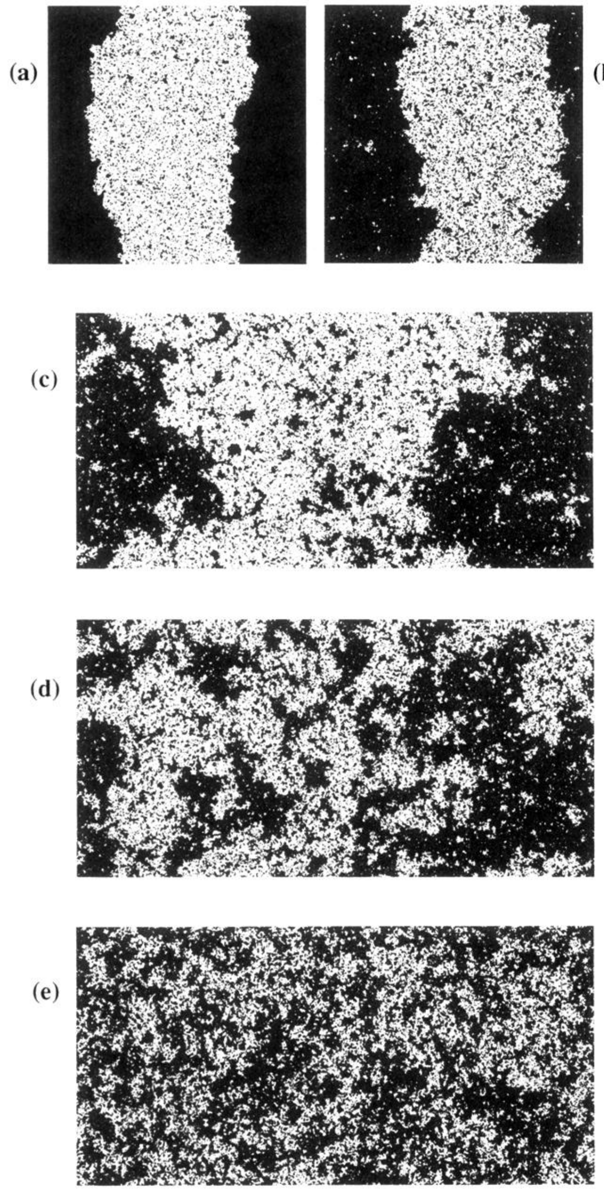

FIG. 2. Snapshots of typical configurations of the catalyst surface for runs of the C-Θ algorithm as described in the text. Black dots represent adsorbed A. Adsorbed B and vacant sites are not shown. (a) 1024×1024 lattice with $P=0$. (b) 1024×1024 lattice with $P=0.030$. (c) 2048×1024 lattice with $P=0.039$. (d) 2048×1024 lattice with $P=0.041$. (e) 2048×1024 lattice with $P=0.050$. The lattices are longer for P near the critical point in order to accommodate larger fluctuations in the phase interface.

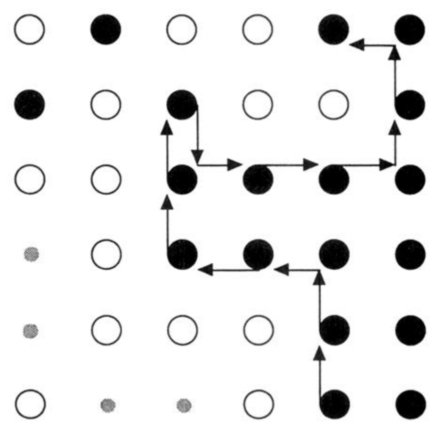

FIG. 3. The arrows show a walk that defines a small section of a sample phase interface, as described in the text. Black dots are adsorbed A, open circles are vacant sites, and small grey dots are adsorbed B. For a walker moving in the direction of the arrows, vacant sites are always to the left, and adsorbed A is always to the right.